Observing the full ocean volume using Deep Argo floats

Nathalie Zilberman, Virginie Thierry, Brian King, Matthew Alford, Xavier Andre, Kevin Balem, Nathan Briggs, Zhaohui Chen, Cécile Cabanes, Laurent Coppola, et al.

frontiers | Frontiers in Marine Science

TYPE Review
PUBLISHED 29 November 2023
DOI 10.3389/fmars.2023.1287867

OPEN ACCESS

EDITED BY
Simone Marini,
National Research Council (CNR), Italy

REVIEWED BY
Xiaogang Xing,
Ministry of Natural Resources, China
Christoph Waldmann,
University of Bremen, Germany

*CORRESPONDENCE
Nathalie V. Zilberman
nzilberman@ucsd.edu

RECEIVED 02 September 2023
ACCEPTED 03 November 2023
PUBLISHED 29 November 2023

CITATION
Zilberman NV, Thierry V, King B, Alford M, André X, Balem K, Briggs N, Chen Z, Cabanes C, Coppola L, Dall'Olmo G, Desbruyères D, Fernandez D, Foppert A, Gardner W, Gasparin F, Hally B, Hosoda S, Johnson GC, Kobayashi T, Le Boyer A, Llovel W, Oke P, Purkey S, Remy E, Roemmich D, Scanderbeg M, Sutton P, Walicka K, Wallace L and van Wijk EM (2023) Observing the full ocean volume using Deep Argo floats.
Front. Mar. Sci. 10:1287867.
doi: 10.3389/fmars.2023.1287867

Observing the full ocean volume using Deep Argo floats

Nathalie V. Zilberman[1*], Virginie Thierry[2], Brian King[3], Matthew Alford[1], Xavier André[4], Kevin Balem[2], Nathan Briggs[3], Zhaohui Chen[5], Cécile Cabanes[2], Laurent Coppola[6,7], Giorgio Dall'Olmo[8], Damien Desbruyères[2], Denise Fernandez[9], Annie Foppert[10], Wilford Gardner[11], Florent Gasparin[12], Bryan Hally[13], Shigeki Hosoda[14], Gregory C. Johnson[15], Taiyo Kobayashi[14], Arnaud Le Boyer[1], William Llovel[2], Peter Oke[16], Sarah Purkey[1], Elisabeth Remy[17], Dean Roemmich[1], Megan Scanderbeg[1], Philip Sutton[9], Kamila Walicka[18], Luke Wallace[13] and Esmee M. van Wijk[10,16]

[1]Integrative Oceanography Division and Climate, Atmospheric Science, and Physical Oceanography Division, Scripps Institution of Oceanography, University of California, San Diego, CA, United States, [2]Univ Brest, CNRS, Ifremer, IRD, Laboratoire d'Océanographie Physique et Spatiale (LOPS), IUEM, F29280, Plouzané, France, [3]National Oceanography Centre, Southampton, United Kingdom, [4]Ifremer, RDT, F29280, Plouzané, France, [5]Key Laboratory of Physical Oceanography/Institute for Advanced Ocean Science/Frontiers Science Center for Deep Ocean Multispheres and Earth System, Ocean University of China, Qingdao, China, [6]Laboratoire d'Océanographie de Villefranche, UMR 7093, CNRS, Sorbonne Université, Villefranche-sur-Mer, France, [7]CNRS, OSU STAMAR, UAR 2017, Sorbonne Université, Paris, France, [8]Sezione di Oceanografia, National Institute of Oceanography and Applied Geophysics, OGS, Trieste, Italy, [9]National Institute of Water and Atmospheric Research, Wellington, New Zealand, [10]Australian Antarctic Program Partnership, Institute for Marine and Antarctic Studies, University of Tasmania, Hobart, TAS, Australia, [11]Department of Oceanography, Texas A&M University, College Station, TX, United States, [12]Université de Toulouse, LEGOS (IRD/UPS/CNES/CNRS), Toulouse, France, [13]University of Tasmania, Hobart, TAS, Australia, [14]Japan Agency for Marine-Earth Science and Technology, Yokosuka, Japan, [15]Pacific Marine Environmental Laboratory, National Oceanic and Atmospheric Administration, Seattle, WA, United States, [16]Environment, Commonwealth Scientific and Industrial Research Organisation (CSIRO), Hobart, TAS, Australia, [17]Operational Oceanography Department, Mercator Ocean International, Toulouse, France, [18]National Oceanography Centre, British Oceanographic Data Centre, Liverpool, United Kingdom

The ocean is the main heat reservoir in Earth's climate system, absorbing most of the top-of-the-atmosphere excess radiation. As the climate warms, anomalously warm and fresh ocean waters in the densest layers formed near Antarctica spread northward through the abyssal ocean, while successions of warming and cooling events are seen in the deep-ocean layers formed near Greenland. The abyssal warming and freshening expands the ocean volume and raises sea level. While temperature and salinity characteristics and large-scale circulation of upper 2000 m ocean waters are well monitored, the present ocean observing network is limited by sparse sampling of the deep ocean below 2000 m. Recently developed autonomous robotic platforms, Deep Argo floats, collect profiles from the surface to the seafloor. These instruments supplement satellite, Core Argo float, and ship-based observations to measure heat and freshwater content in the full ocean volume and close the sea level budget. Here, the value of Deep Argo and planned strategy to implement the global array are described.

Additional objectives of Deep Argo may include dissolved oxygen measurements, and testing of ocean mixing and optical scattering sensors. The development of an emerging ocean bathymetry dataset using Deep Argo measurements is also described.

KEYWORDS

deep ocean, ocean observation, ocean heat content (OHC), sea level (SL), ocean deoxygenation, bathymetry accuracy, ocean mixing, sediment transport

1 Introduction

Earth's Energy Imbalance (EEI), the rate of net solar energy absorbed by the Earth, shows an increased trend in the past two decades at least partly as a result of increased atmospheric greenhouse gases (GHG; Loeb et al., 2021). Unless GHG emissions are sharply reduced, global warming is likely to exceed 1.5-2°C above pre-industrial levels. The 1.5°C threshold was recognized in the Paris Agreement as synonymous with extreme weather events, warmer ocean waters, and sea level rise, threatening human safety and ecosystem health (Allen et al., 2019). Due to its high heat capacity, the ocean delays the atmospheric warming, absorbing about 90% of the EEI (von Schuckmann et al., 2023). Together, the expansion of seawater from increasing temperature, import of continental water from Greenland and Antarctic ice sheet mass loss, and the melt of mountain glaciers, have resulted in a global mean sea level (GMSL) rise of 15-25 cm over 1901-2018 (1.28 to 2.17 mm per year; Fox-Kemper et al., 2021). The rate of rise has accelerated in the past two decades (Nerem et al., 2018) and reached 3.58 ± 0.25 mm per year over 2005-2015 (Llovel et al., 2019). Model projections indicate that this acceleration is likely to continue through the century (Fox-Kemper et al., 2021), increasing the extent and severity of flooding and coastal erosion (Martyr-Koller et al., 2021). Current estimates of global ocean heat content (OHC) inferred from sea-going platforms and sea level change assessed from satellite altimetry, lack the desired spatial resolution and precision to generate accurate projections of EEI response to climate policies (Meyssignac et al., 2019; Palmer, 2017; WCRP Global Sea Level Budget Group, 2018).

While the ocean sampling of the upper 2000 m has dramatically increased due to the revolutionary contributions of autonomous platforms, the status of deep-sea observing has remained fragmentary (Meyssignac et al., 2019; von Schuckmann et al., 2023) and opportunistic. Although the deep ocean below 2000 m represents half of the total ocean volume, only 10% of historical temperature and salinity profiles extend below 2000 m (Garcia et al., 2019). Because deep-ocean measurements are unevenly distributed in space and time, regional-to-global and seasonal-to-interannual variations are poorly resolved, and spurious patterns of ocean temperature and salinity fluctuations can occur (Johnson and Lyman, 2020). Global decadal variations in deep-ocean volume due to temperature (thermosteric) changes contribute 10% of the GMSL budget (Chang et al., 2019) but the impact is significantly higher (~30%) in the Southern Ocean where abyssal warming is strongest (Purkey and Johnson, 2010). The GMSL budget closes between 2005 and 2015 when using an approximate estimate of decadal variation of the ocean volume due to density (steric) changes (Llovel et al., 2019; Chen et al., 2022), but appears no longer closed between 2016 and 2019 (Chen et al., 2020). While part of the non-closure of the GMSL budget after 2015 can be explained by salty drift of conductivity-temperature-depth (CTD) sensors on some Argo floats, potential drift of satellite altimeters, and noise contamination of Gravity Recovery and Climate Experiment (GRACE/GRACE-FO) accelerometer measurements, the sparse sampling of the deep ocean, especially in the Southern Hemisphere, is likely another contributor (Barnoud et al., 2021). Even during 2005-2015 when the sea level budget closes at the global scale, a mismatch between sea level from altimetry and the sum of GRACE mass addition, Argo upper-ocean steric sea level, and shipboard deep-ocean steric sea level is observed at local to sub-basin scale (Royston et al., 2020).

General circulation models are essential tools to monitor and forecast the influence of ocean-atmosphere coupling on weather and climate (Stammer et al., 2019; Lellouche et al., 2021), but model drift in the deep ocean limits their ability to predict ocean heat and freshwater content (Palmer et al., 2011). Correction techniques developed to force model fields towards specific deep-ocean conditions have shown discrepancies in simulated ocean temperature and salinity compared with observations (Uotila et al., 2019). The addition of global and frequent deep-ocean observations improves the representation of deep-ocean processes and can prevent unrealistic drifts (Palmer, 2017). Furthermore, deep-ocean observations decrease uncertainties in water mass properties (Gasparin et al., 2019; Gasparin et al., 2020), reduce bias in upper-ocean decadal predictability (e.g., Sévellec and Fedorov, 2013; Levin et al., 2019), and improve the consistency of assimilated *in situ* and satellite observations (Abdalla et al., 2021).

Partly owing to the decrease in oxygen solubility with ocean warming, dissolved oxygen (DO) concentrations have decreased (Schmidtko et al., 2017) and oceanic regions with low-oxygen concentration, termed quasi-permanent oxygen minimum zones (OMZs), have grown over the last five decades. The spread of these inhospitable areas decreases biological diversity, reduces physiological adaptation, and depletes fish stocks (Garçon et al., 2019). Earth model simulations predict an expansion of OMZs (Busecke et al., 2022) and intensification of oxygen decline from the

surface to abyssal depths in the next decade (Kwiatkowski et al., 2020). Due to the scarcity of deep-ocean oxygen observations, the response of low-oxygen habitat size and distribution to physical and biogeochemical processes remains poorly understood (Levin, 2018; Oschlies et al., 2018), and the ability of marine biogeochemical models to simulate the response and feedback of marine ecosystems to climate change is limited (Séférian et al., 2020).

Deep Argo is an ongoing expansion of the Argo Program using autonomous robotic floats with the ability to cycle between the surface and the seafloor every 10 days, and transmit data via satellites (Roemmich et al., 2019a). Deep Argo is the deep component of the OneArgo design, endorsed by the U.N. Ocean Decade (Owens et al., 2022). At present, there are ~200 Deep Argo floats sampling some of the deepest regions of the ocean (Figure 1). The Argo community recommends increasing the number of active deep floats to form a 5° x 5° global array of 1200 Deep Argo floats in the seasonally ice-free global ocean deeper than 2000 m. The capacity of the fully-implemented Deep Argo array to reduce errors in decadal trends of deep OHC and deep-ocean thermal expansion (Johnson et al., 2015; Meyssignac et al., 2019) is recognized by the EEI community (von Schuckmann et al., 2020; von Schuckmann et al., 2023) and the World Climate Research Program (WCRP) global sea level budget group (WCRP Global Sea Level Budget Group, 2018; Cazenave et al., 2019). Other benefits of Deep Argo are to establish relationships between fluctuations of the deep meridional overturning circulation and changes in ocean temperature and salinity and their representations in ocean reanalyzes and forecasts (Gasparin et al., 2020). The value of adding sensors on Deep Argo floats to assess full-depth ocean oxygen content, mixing, and sediment transport, and the capacity of Deep Argo floats to improve global ocean bathymetry are under study. Deep Argo floats are expected to play a key role in the Deep Ocean Observing Strategy (DOOS) initiative, a growing effort by the scientific community to improve the deep-ocean observing system (Levin et al., 2019).

2 Requirements and technology status

2.1 Float and sensor requirements

In accordance with Argo's practices, Deep Argo data are shared publicly in near real-time, usually in less than 24 hours. A further quality-controlled version is made available within 6 months on the two Argo Global Data Assembly Centers (GDAC) in netCDF files, as well as inserted onto the Global Telecommunications System (GTS) in the Binary Universal Form for the Representation (BUFR) format. For consistency with the Core Argo mission, Deep Argo floats operate on a nominal 10-day cycle between the surface and the seafloor (4000-m or 6000-m depth, depending on the float model). For Deep Argo floats profiling on descent and ascent, measurements on ascent should be collected at least in the upper 1000 m to provide near real-time data to ocean forecasting and seasonal prediction communities.

Required accuracies for Deep Argo salinity, temperature, and pressure measurements are to approach ±0.002 PSS-78, ± 0.001°C, and ±3 dbar respectively (Roemmich et al., 2019a), in line with shipboard measurements from the Global Ocean Ship-Based Hydrographic Investigations Program (GOSHIP; Katsumata et al., 2022). It is recommended that technology development continues to reach targeted values. With salinity accuracy target five times more stringent than Core (0-2000 m) Argo (Wong et al., 2020), Deep Argo can efficiently supplement the high-quality shipboard reference database used for Core Argo quality control and has therefore the capacity to improve the post-calibration of salinity measurements. The accuracy, precision, and vertical resolution of

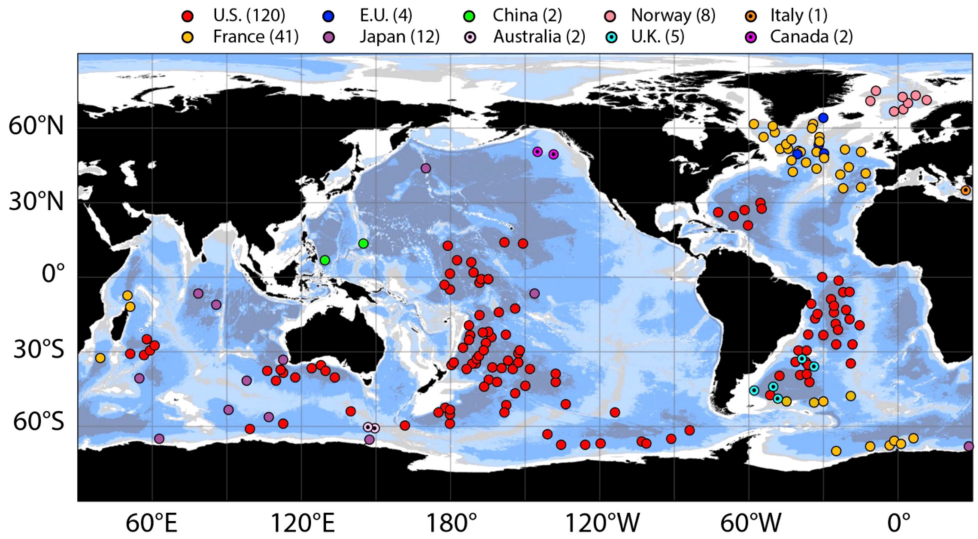

FIGURE 1
Locations of the 197 Deep Argo floats active in May 2023. This figure shows locations of 4000 m capable Deep Arvor and Deep NINJA, and 6000 m capable Deep SOLO and Deep APEX floats, color coded by national program. The background colors indicate ocean bottom depth: <2000 m (white), 2000-3000 m (light gray), 3000-4000 m (light blue), 4000-5000 m (blue), and >5000 m (dark gray). Data courtesy of OceanOPS.

the Deep Argo CTD sensor influence the temperature-salinity relation, and estimates of steric height and vertical stratification as outlined below.

Steric height is vital for sea level budget analyses (Cazenave et al., 2019) as well as geostrophic circulation studies (Zilberman et al., 2020). Errors the size of Deep Argo target accuracies (± 0.002 PSS-78, ± 0.001°C, and ±3 dbar) applied to full-depth (0–6000 m) profiles at 20°S in the Brazil Basin result in sea level errors of about ±0.9, ± 0.1, and ±0.06 cm, as well as depth-integrated transport errors (assuming zero velocity at the bottom) of ±5.1, ± 0.6, and ±1.5 10^6 m^3 s^{-1} for salinity, temperature, and pressure, respectively. With these targeted values, salinity accuracy has the largest impact on sea level, geostrophic velocity, and transport error budgets.

Mean temperature-salinity relations are used to diagnose deep water-mass distributions (Johnson, 2008) and ocean circulation (Zilberman et al., 2020), and their variations are important in monitoring changes in deep and bottom water properties and formation rates (Purkey et al., 2019). Again, salinity accuracy is likely the limiting factor, but decadal changes in the temperature-salinity relationships of Antarctic Bottom Water (e.g. van Wijk and Rintoul., 2014) and the constituents of North Atlantic Deep Water (Yashayaev, 2007) near their sources are several times Deep Argo target accuracies, and therefore easily quantifiable.

Stratification variations on small vertical scales are needed to estimate mixing related to internal waves and tides (Whalen et al., 2012), while vertical stratification on longer length scales is appropriate to study features such as variability in the pycnocline between deep and bottom waters, which may change ocean mixing and diffusion rates (Zhang et al., 2021). For compatibility with Core Argo sampling recommendation in the upper 2000 m, Deep Argo float longevity, and ocean mixing parameterizations, the recommended vertical resolution of Deep Argo profiles is 2-dbar bin-averaging in the upper 2000 m, and may increase to 10-dbar, or even 25-dbar, vertical resolution below 2000 m.

2.2 Readiness of float and sensor technology

Deep Argo float technology has been extensively tested in regional pilot arrays (Figure 1). Several float designs have proven their ability to collect deep-ocean profiles to 4000 m (e.g., Deep NINJA and Deep Arvor) and 6000 m (e.g., Deep SOLO and Deep APEX) (Kobayashi et al., 2013; Petzrick et al., 2014; Le Reste et al., 2016; Roemmich et al., 2019b) and new float designs are under development to further increase the diversity of the Deep Argo fleet.

Deep Argo CTD sensor specifications of temperature, salinity, and pressure accuracies approach the targeted values described in section 2.1, and specifications of stability are compatible with the Deep Argo targets. Both extended-depth SBE41-CP and SBE61 models from SeaBird Scientific (SBS) are operational. A pilot Deep Argo CTD instrument from RBR is under testing. The ability of the SBE61 to reach the targeted temperature accuracy of ±0.001°C has been demonstrated from comparisons of shipboard rosette-mounted SBE-61 CTDs with shipboard (SBE-911) CTD observations (Roemmich et al., 2019a). Work has been achieved to improve our understanding of the impact of temperature and pressure variations on conductivity and pressure measurements (Kobayashi et al., 2021). A compressibility correction of the conductivity cell used on the extended-depth SBE41-CP and SBE61 has been successfully implemented, reducing salinity bias observed in the field from comparisons of Deep Argo-mounted extended-depth SBE41-CP and SBE-61 with shipboard reference profiles to ±0.002 PSS-78 (Foppert et al., 2021; Walicka et al., 2022), consistent with the Deep Argo target. Once the pressure dependent salinity bias is adjusted, a time-varying correction of salinity can be applied as long as salinity drift is linear in time (Owens and Wong, 2009; Cabanes et al., 2016). A description of quality control procedures and best practices for analysis of Deep Argo temperature, salinity and pressure is provided in the report by Walicka et al. (2022). New pressure sensors with accuracy and stability specifications exceeding the Deep Argo target are undergoing testing in the field. Although reaching the ambitious accuracy targets described in section 2.1 across all Deep Argo CTD sensors is a challenging task, ongoing work is showing great potential for success. To that end, it is essential that research institutions continue independent assessment of sensor accuracy and stability, the sensor's ability to maintain targeted accuracy over the float lifetime, using Deep Argo float comparisons with high-quality shipboard reference data, and maintain collaborative work with the industry to optimize calibration and data quality control procedures. Maintaining a diversity of distinct Deep Argo floats and sensors from several manufacturers is encouraged to avoid supply chain issues, and to effectively identify, understand, and resolve potential float and sensor failure.

3 Value of Deep Argo data

The amount of deep-ocean profiles collected from Deep Argo floats in the South Australian, Australian Antarctic, Southwest Pacific, and Brazil basins in less than 7 years approaches that of deep-ocean data accumulated from ships over the past 70 years (Figure 2). This new dataset has enabled breakthroughs in our understanding of OHC, ocean circulation, and sea level change.

For instance, strong decadal-scale warming rates of the cold and dense Antarctic Bottom Water (AABW) that spreads over much of the abyssal ocean (depth > 4000 m) have been quantified combining Deep Argo data with historical data in the Brazil Basin (Johnson et al., 2020), and Argentine Basin (Johnson, 2022) with trend estimates that are up-to-date and several times more certain than those from repeat hydrography alone (Figures 3A, B). Deep Argo data alone are measuring shorter time-scale trends, such as accelerated warming in the bottom waters of Southwest Pacific Basin since 2014 (Johnson et al., 2019), with increasing certainty as the record length increases (Figure 3C). Other scientific advances using Deep Argo data with other data sources include a warming-to-cooling reversal of the Lower North Atlantic Deep Water observed in the subpolar North Atlantic in the mid-2010s (Desbruyères et al., 2022; Figure 3D).

Small clusters of Deep Argo floats have demonstrated their ability to detect the reversal of a long-term freshening trend in the

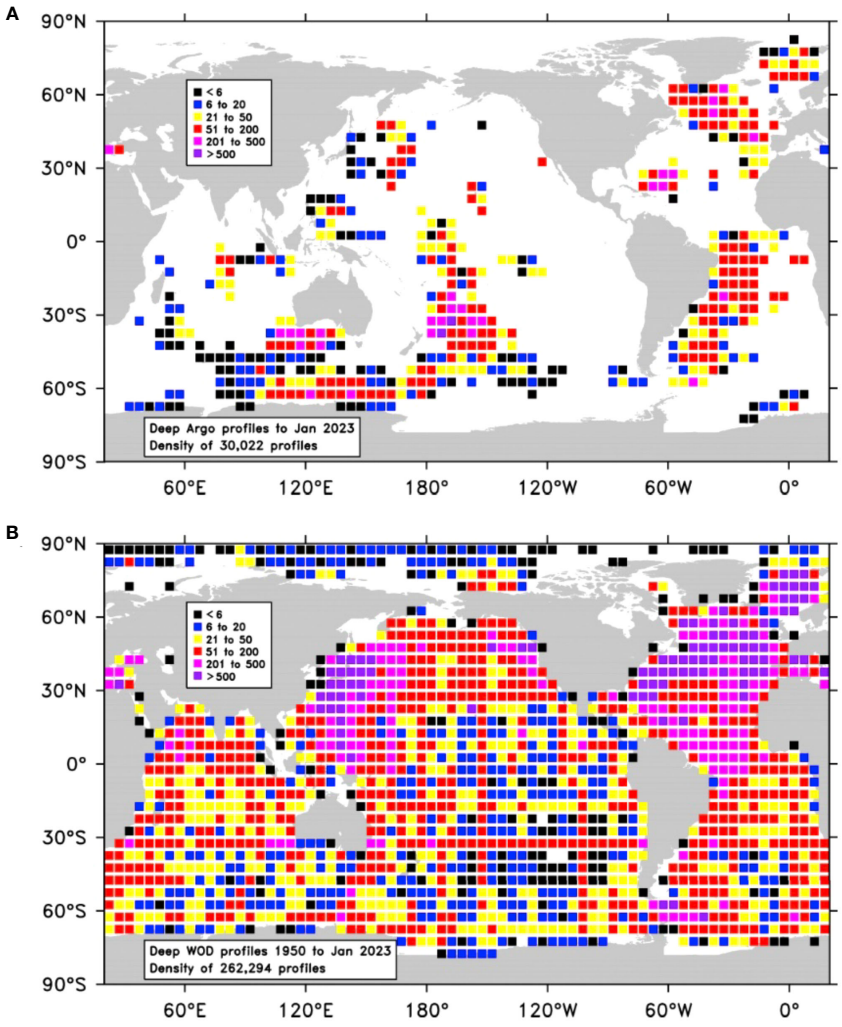

FIGURE 2
The sampling density per 5° latitude by 5° longitude of temperature and salinity profiles deeper than 2000 m. **(A)** Deep Argo profiles in regional pilot arrays deployed between 2014 and 2023. **(B)** Historical non-Argo profiles from the World Ocean Database (WOD) 2018 collected between 1950 and 2023 (Garcia et al., 2019).

Australian Antarctic Basin, at higher temporal and spatial resolution than historical shipboard CTD occupations (Thomas et al., 2020; Foppert et al., 2021). By providing simultaneous temperature and salinity profiles over broad swaths of ocean basins, Deep Argo has proven effective at mapping large-scale circulation pathways of dense water masses formed near Antarctica (Thomas et al., 2020; Foppert et al., 2021), in the subpolar North Atlantic Ocean (Racapé et al., 2019; Petit et al., 2022), and in the Southwest Pacific Ocean (Zilberman et al., 2020; Figures 4A, B) with unprecedented detail. Seasonal fluctuations in the recirculation of the Deep Western Boundary Current of the Southwest Pacific Basin, and associated forcing mechanisms, were detected for the first time (Zilberman et al., 2020; Figures 4C), as was a slowdown of flow of AABW into the Argentine Basin (Johnson, 2022). In the North Atlantic Ocean, Deep Argo profiles have been added to the *In Situ* Analysis System (ISAS, Gaillard et al., 2016; Kolodziejczyk et al., 2021) to provide monthly gridded fields of full-depth temperature and salinity, and to improve estimates of subannual-to-annual full-depth regional steric sea level change. Deep Argo data have even been used to describe regional patterns of deep internal wave activity (Johnson, 2022).

The fully implemented global Deep Argo 1200-float array will diminish the spread in plausible regional-to-basin-scale OHC trends of the deep ocean due to sparse historical sampling, while filling temporal gaps at subseasonal to interannual time scales not often sampled by repeat hydrographic sections (Desbruyères et al., 2016). Deep Argo thermosteric and halosteric sea level sampling will decrease the observed regional-to-basin-scale mismatch between sea level from altimetry and the sum of GRACE mass addition, Argo upper-ocean steric sea level, and shipboard deep-ocean steric sea level (Royston et al., 2020). Deep Argo has the capacity to reduce errors in global decadal trends of deep OHC from ±0.04 to ±0.006 W m^{-2} (Meyssignac et al., 2019) and deep-ocean thermal expansion from ±0.73 to ±0.1 mm $decade^{-1}$ (Johnson et al., 2015; Desbruyères et al., 2016). As the array expands, Deep Argo will become increasingly useful to improve knowledge of the

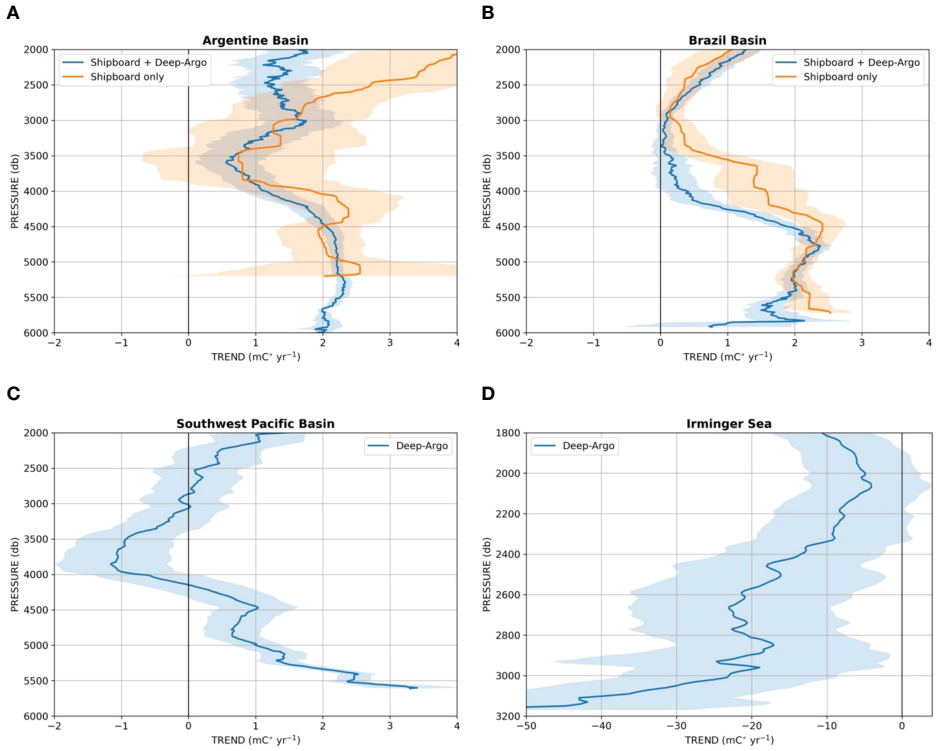

FIGURE 3
Mean deep-ocean temperature trends using Deep Argo. Temperature trends are shown in (m°C yr^{-1}) vs. pressure (lines) with 5–95% confidence limits (shading). **(A)** Temperature trends in the Argentine Basin computed by comparing all pairs of Deep Argo temperature profiles collected from January 2021 to April 2023 with nearby historical profiles collected from 1972 to 1998 (blue, updated following Johnson, 2022) and computed from repeat hydrography sections carried out in the Argentine Basin between the early 1990's and the mid-2010's (orange, from Desbruyères et al, 2016). **(B)** Temperature trends in the Brazil Basin computed by comparing all pairs of Deep Argo profiles reported from May 2019 to April 2023 within nearby WOCE profiles from 1989-1995 (blue, updated following Johnson et al., 2021) and computed from repeat hydrography sections carried out in the Brazil Basin between the early 1990's and the mid-2010's (orange, from Desbruyères et al., 2016). **(C)** Temperature trends in the Southwest Pacific Basin evaluated from Deep Argo data collected from June 2014 to April 2023 (updated from Johnson et al., 2019). **(D)** Temperature trends in the Irminger Sea evaluated from Deep Argo during 2016 – 2021 (from Desbruyères et al., 2022). This last trend is density-compensated and only the layer > 36.94 m^{-3} occupied by Lower North Atlantic Deep Water is considered (note the different x-axis scale).

regional-to-basin-scale structure and subseasonal-to-interannual fluctuations of the large-scale deep-ocean circulation, and advance understanding of the drivers for these changes. In particular, Deep Argo will provide a new means to validate numerical model projections of the impact of meltwater release from Greenland and Antarctica on the deep-ocean overturning circulation (Swingedouw et al., 2022; Li et al., 2023; Zhou et al., 2023).

4 Global implementation

To be sustainable, it is essential that the global implementation of the Deep Argo array stems from achievable long-term resources of international Argo partners and production capability of the float and sensor manufacturers. Since each Deep Argo float replaces a Core Argo float in the OneArgo design (Roemmich et al., 2019a; Owens et al., 2022), a minimum lifetime of at least 4 years, approaching the averaged 5.5-year Core Argo float longevity, is desired across all Deep Argo float models (Zilberman et al., 2019). Assuming an averaged Deep Argo float longevity of 4 years, implementing a 1200-float global array size would require 300 float deployments per year among all international partners. Some active Deep Argo float models have already achieved a longevity exceeding 5 years. Engineering advances will continue to increase the averaged Deep Argo float lifetime in order to reduce the size of annual float deployments needed to re-seed the array. The fully implemented Deep Argo array will require additional support from international Deep Argo partners as the averaged capital purchase of Deep Argo floats across all active models is two to three times that of Core Argo. The data quality control and deployment costs for Deep and Core Argo floats are similar.

Additional recommendations should be considered in order to optimize deep-ocean sampling cost and efficiency. Prior to reaching the 1200-float design target, Deep Argo float deployments should prioritize deep (> 2000 m) regions of the subpolar North Atlantic, Southern Ocean, and tropical oceans, and abyssal (> 4000 m) plains of the ocean interior, where highest deep-ocean temperature fluctuations have been observed. Deep Argo floats deployed in these regions may park at depths greater than 1000 m to minimize float dispersion, hence optimizing their value. For instance, programming parking depth to coincide with reduced background flow such as within 500-m above the seafloor in abyssal plains, and

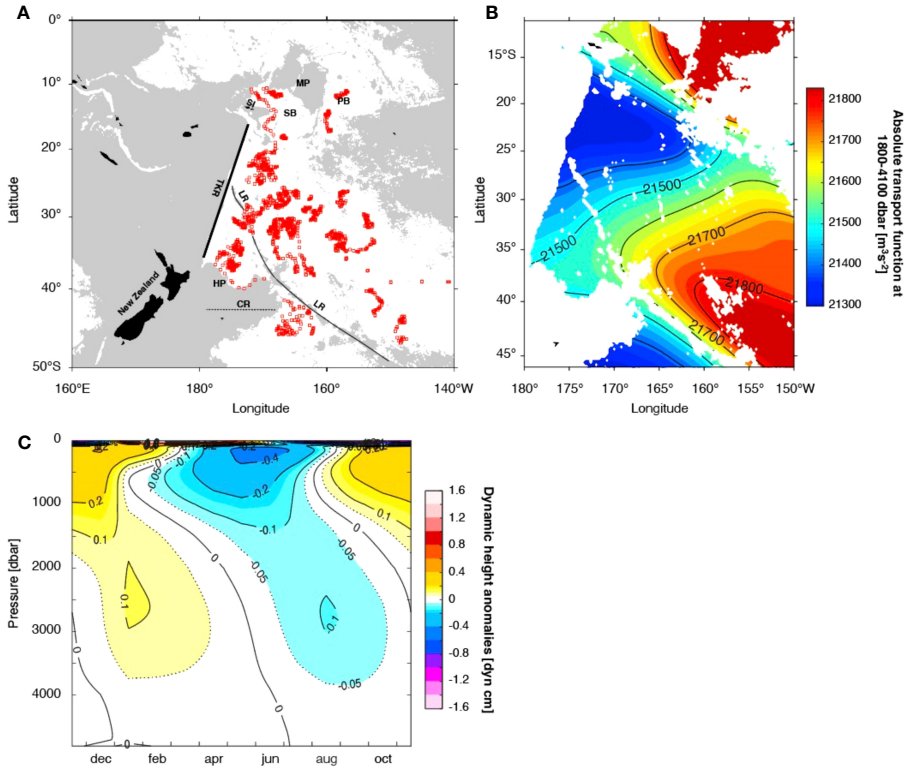

FIGURE 4
Spatial structure and seasonal variability of the deep-ocean circulation in the Southwest Pacific Ocean using Deep Argo. **(A)** Positions of Deep Argo profiles collected from January 2016 to December 2019 are indicated in squared red symbols. The shaded gray color indicates bottom depth shallower than 4800-m depth, and the white background color shows regions deeper than 4800 m. The Samoan Islands (SI), Samoan Basin (SB), Manihiki Plateau (MP), Penrhyn Basin (PB), Louisville Ridge (LR, thin black line), Tonga Kermadec Ridge (TKR, thick black line), Hikurangi Plateau (HP), Chatham Rise (CR, dashed black line), and New Zealand are indicated (from Zilberman et al., 2020). **(B)** Absolute transport function integrated between 1800 and 4100 dbar for 2016–2019. The white background color indicates regions shallower than 4800 m (from Zilberman et al., 2020). **(C)** Seasonal variability of dynamic height referenced to 4800 dbar between 0 and 4800 dbar between 46° and 11°S for 2016–2019 (from Zilberman et al., 2020).

above deep boundary currents near topography, has proven an effective way to limit horizontal displacement during parking (Zilberman et al., 2020). Floats may also be programmed to park at the core depth of local deep water masses in order to assess regional circulation (Racapé et al., 2019). Once a global array is achieved, it is recommended that all Deep Argo floats should park at 1000 m in order to facilitate homogeneous float sampling (Roemmich et al., 2019a) and increase the velocity database from Argo float trajectories to reduce sampling error (Zilberman et al., 2023).

5 Ongoing evolution of the Deep Argo array

Sensors to measure ocean properties additional to temperature, salinity, and pressure are under testing to assess their performance in the field and increase value of the Deep Argo data set. Any additional sensors should be compatible with the Deep Argo float longevity target and should not impede the achievement of a global Deep Argo array. The opportunistic measurement of bathymetry from Deep Argo floats, which does not require supplementary sensor measurements, is under evaluation.

5.1 Dissolved oxygen

Full-depth Deep Argo DO data can help constrain oceanic sources and sinks of oxygen (Riser and Johnson, 2008) and provide better assessments and predictions of global ocean deoxygenation (Schmidtko et al., 2017). Combined with Deep Argo temperature and salinity, DO measurements can improve our understanding of water-mass formation (e.g., Johnson, 2008), ocean ventilation (Piron et al., 2016), ocean circulation and mixing (Racapé et al., 2019) and the impact of these processes on oxygen change in the deep ocean (Coppola et al., 2017; Ulses et al., 2021). Using temperature, salinity, and DO in transfer functions allows estimates of concentrations of nutrients, carbonate system parameters (Sauzède et al., 2017), and ultimately anthropogenic carbon storage and export. About 30% of active Deep Argo floats are equipped with DO sensors. The best accuracy reached in the field by Deep Argo DO sensors is 1-2 µmol kg^{-1} and requires a careful correction of the data to account for sensor drift (Bittig et al., 2018; Bittig et al., 2019), time response (Gordon et al., 2020) and pressure dependent response of the sensor (Bittig et al., 2018; Racapé et al., 2019). The current accuracy of Deep Argo DO sensors is suitable for all the above-mentioned applications, but needs to be increased to 0.5 µmol kg^{-1} to resolve deoxygenation trends (Grégoire et al, 2021).

Work is underway to bring DO accuracy to this target and to determine through observing system simulation experiments (OSSEs) an optimal deployment strategy, and the required amount of Deep Argo floats equipped with DO sensors. Deep Argo will supplement DO data from repeat shipboard hydrography (Testor et al., 2018), and in return, shipboard observations will help validate and calibrate Deep Argo profiles (Racapé et al., 2019). It is expected that Deep Argo floats with DO sensors could play a key role in the expansion of the Global Ocean Oxygen Database and Atlas (Grégoire et al, 2021).

5.2 Bathymetry

Ocean bathymetry has a fundamental impact on the pathway and strength of ocean currents (Wilson et al., 2022), and amplitude of ocean mixing (Mashayek et al., 2017), and can influence heat and freshwater exchange between the ocean and atmosphere (de Boer et al., 2022). Variations in the shape of the seafloor can dictate the magnitude and frequency of earthquakes (Passarelli et al., 2022) and the generation and propagation of tsunamis (Salaree and Okal, 2020). Less than 24% of the seafloor topography from the General Bathymetric Chart of the Ocean (GEBCO) dataset is constrained by shipboard sounding measurements or other direct measurements, and is limited mostly to Exclusive Economic Zones (Tozer et al., 2019; Wölfl et al., 2019; GEBCO Bathymetric Compilation Group, 2022). Deep Argo floats are not equipped with an echosounder, but bottom depth can be estimated when near-constant pressure values are recorded over a set period of time when the float contacts the seafloor. The main challenge in estimating Argo-based bathymetry is the horizontal displacement that occurs between the grounding position at depth and the position obtained at the surface, once a connection between the float and satellite positioning system is established (Ollitrault and Rannou, 2013). Estimated horizontal errors using the Bluelink ReANalysis 2020 (BRAN2020; Chamberlain et al., 2021) and GLobal Ocean ReanalYsiS (GLORYS12; Lellouche et al., 2021) ocean reanalyzes are 1-2 km in widespread regions of the deep-ocean interior, 2-8 km in equatorial regions, and reach 8-18 km at ocean western boundaries and near topography where ocean currents are strongest. Preliminary comparisons between historical Argo and GEBCO bathymetry sourced from echo sounding measurements show encouraging agreement (van Wijk et al., 2022). Based on the averaged Deep Argo float grounding rate of 60% over the past 4 years, a 1200-float array could contribute over 25,000 additional deep-ocean bathymetry measurements every year to global bathymetry datasets such as the Nippon Foundation – GEBCO Seabed 2030 Project (Mayer et al., 2018).

5.3 Ocean mixing

Ocean mixing controls the vertical transport of water masses within the meridional overturning circulation and therefore strongly affects the oceanic uptake of heat, oxygen, and anthropogenic carbon (Cimoli et al., 2023). Upcoming work includes testing the ability of pilot temperature and velocity shear microstructure sensors mounted on Deep Argo floats to improve deep-ocean mixing estimates. At present, deep ocean mixing is measured from either extremely sparse focused process studies using tracer, moorings, and microstructure measurements (Waterhouse et al., 2014; Ferron et al., 2017; MacKinnon et al., 2017) or from fine-scale parameterizations using Argo and ship-based CTD profiles (Whalen et al., 2015; Ferron et al., 2016). However, these parametrizations rely on assumptions that may not be valid for all ocean dynamics (Vladoiu et al., 2021) leading to systematic biases in some areas of the ocean (Lele et al., 2021), particularly close to seafloor topography. Modern turbulent packages offer low-power, inexpensive options (e.g., Le Boyer, 2021) that have already successfully been integrated onto upper 2000 m ocean observing platforms (e.g., Nagai et al., 2015). The slow profiling speeds of Deep Argo floats and limited turbulence noise induced by the float-sensor apparatus, coupled with new technology and vetted onboard processing (e.g., Hughes et al., 2023) have reduced the amount of transmitted data required to compute mixing estimates reliably.

5.4 Optical scattering

Deep scattering measurements are needed to improve our understanding of the fate of sinking particles produced at the surface and their role in burying organic carbon in sediments, to quantify sediment resuspension and transport near the ocean bottom, and to measure transport and redistribution of trace metals (Lam and Bishop, 2008; Estapa et al., 2015). Another application of deep-ocean scattering data is to assess the environmental impacts of deep-sea mining by establishing a baseline for the concentration of particles present below 2000 m and inferring variations from this baseline due to mining operations. Emerging plans involve testing the performance of pilot optical scattering sensors (Gardner et al., 2018) on Deep Argo floats to measure the concentration of particles present in deep-sea water. Deep-rated optical scattering sensors are commercially available and have been field tested to 6000 m (e.g., Gardner et al., 2018; Ray et al., 2020), but have not yet been implemented on Deep Argo floats. The high sensitivity of optical scattering to minerals and large particles (Briggs et al., 2020) implies that no increase in sensor sensitivity nor accuracy is needed to quantitatively resolve the deep-ocean signal. Sensor calibration and data quality control will be studied to address and correct the effect of pressure cycling on the accuracy and stability of optical scattering measurements (Hu et al., 2019).

6 Conclusion

Deep Argo floats are autonomous profilers with limited carbon footprint and environmental impact, and are rapidly improving deep-ocean sampling coverage. A strategy to implement the global 1200 Deep Argo float array has been carefully designed to resolve regional-to-global variations of temperature and salinity over the full-ocean depth at subseasonal-to-decadal time scale. Ongoing challenges are to increase the diversity of Deep Argo floats and CTD sensor models, extend the averaged Deep Argo float longevity to > 4 years, improve sensor performance and refine real-time and delayed-mode Deep Argo data quality control procedures to achieve targeted values of temperature, salinity, and pressure accuracies across all CTD sensors. Concurrent observations from Core and Deep Argo, repeat hydrography, and

satellite networks will enable identification and correction of bias and drift in sea level anomalies measured from satellite altimeters, ocean mass addition from space gravimetry, and salinity measurements from Argo CTD sensors. The deployment of the global Deep Argo array, combined with Core Argo, repeat hydrography and satellite altimetry and gravimetry missions, has the capacity to improve assessments and projections of the global planetary heat, freshwater, and sea level budgets, and strength of the overturning circulation. While Deep Argo's priority is the full implementation of the backbone 1200-float array extending Argo temperature and salinity profiling to the abyssal ocean, emerging projects are under evaluation to address ocean deoxygenation and carbon sequestration, ocean mixing, sediment transport, and improve bathymetry estimates.

Author contributions

NZ: Conceptualization, Investigation, Writing – original draft, Writing – review and editing. VT: Investigation, Writing – original draft, Writing – review and editing. BK: Writing – review and editing. MA: Writing – review and editing. XA: Writing – review and editing. KB: Writing – review and editing. NB: Writing – review and editing. ZC: Writing – review and editing. CC: Writing – review and editing. LC: Writing – review and editing. GD'O: Writing – review and editing. DD: Writing – review and editing. DF: Writing – review and editing. AF: Writing – review and editing. WG: Writing – review and editing. FG: Writing – review and editing. BH: Writing – review and editing. SH: Writing – review and editing. GJ: Writing – review and editing. TK: Writing – review and editing. AL: Writing – review and editing. WL: Writing – review and editing. PO: Writing – review and editing. SP: Writing – review and editing. ER: Writing – review and editing. DR: Writing – review and editing. MS: Writing – review and editing. PS: Writing – review and editing. KW: Writing – review and editing. LW: Writing – review and editing. EW: Writing – review and editing.

Funding

The author(s) declare financial support was received for the research, authorship, and/or publication of this article. The authors gratefully acknowledge financial support by the following projects and grants: NZ was supported by NOPP (NOAA grant NA18OAR0110434) and NSF (OCE-2242742). NZ, SP, DR and MS received support from NOAA Global Ocean Monitoring and Observing Program through Award NA20OAR4320278. GJ was supported by the NOAA Global Ocean Monitoring and Observation Program and NOAA Research. VT, XA, KB, CC and DD were supported by the Ifremer PIANO project and by the Equipex+ Argo-2030 project that received support from the French government within the framework of the "Investissements d'avenir" program integrated in France 2030 and managed by the Agence Nationale de la Recherche (ANR; grant ANR-21-ESRE-0019). EW was supported by the Australian Antarctic Program Partnership. BH was supported by funding from the Australian Hydrographic Office, Australian Government. LW was supported by the University of Tasmania, Hobart, TAS, Australia.

Acknowledgments

Argo data were collected and made freely available by the International Argo Program and the national programs that contribute to it. (https://argo.ucsd.edu, https://www.ocean-ops.org). The Argo Programme is part of the Global Ocean Observing System. Thanks to Pauline Weatherall, Thierry Schmitt, Kevin Mackay, Brook Tozer, and David Sandwell for providing helpful insight on the GEBCO bathymetric dataset.

Conflict of interest

The authors declare that the research was conducted in the absence of any commercial or financial relationships that could be construed as a potential conflict of interest.

Publisher's note

References

Abdalla, S., Kolahchi, A. A., Ablain, M., Adusumilli, S., Bhowmick, S. A., Alou-Font, E., et al. (2021). Altimetry for the future: Building on 25 years of progress. *Adv. Space Res.* 68 (2), 319–363. doi: 10.1016/j.asr.2021.01.022

Allen, M., Antwi-Agyei, P., Aragon-Durand, F., Babiker, M., Bertoldi, P., Bind, M., et al. (2019). Technical Summary: Global warming of 1.5°C. An IPCC Special Report on the impacts of global warming of 1.5°C above pre-industrial levels and related global greenhouse gas emission pathways, in the context of strengthening the global response to the threat of climate change, sustainable development, and efforts to eradicate poverty. *Intergovernmental Panel Climate Change.*

Barnoud, A., Pfeffer, J., Guérou, A., Frery, M.-L., Siméon, M., Cazenave, A., et al. (2021). Contributions of altimetry and Argo to non-closure of the global mean sea level budget since 2016. *Geophysical Res. Lett.* 48, e2021GL092824. doi: 10.1029/2021GL092824

Bittig, H. C., Körtzinger, A., Neill, C., van Ooijen, E., Plant, J. N., Hahn, J., et al. (2018). Oxygen optode sensors: principle, characterization, calibration, and application in the ocean. *Front. Mar. Sci.* 4. doi: 10.3389/fmars.2017.00429

Bittig, H., Maurer, T., Plant, J., Schmechtig, C., Wong, A., Claustre, H., et al. (2019). A BGC-argo guide: planning, deployment, data handling and usage. *Front. Mar. Sci.* 6. doi: 10.3389/fmars.2019.00502

Briggs, N., Dall'Olmo, G., and Claustre, H. (2020). Major role of particle fragmentation in regulating biological sequestration of CO_2 by the oceans. *Science* 367 (6479), 791–793. doi: 10.1126/science.aay1790

Busecke, J. J. M., Resplandy, L., Ditkovsky, S. J., and John, J. G. (2022). Diverging fates of the Pacific Ocean oxygen minimum zone and its core in a warming world. *AGU Adv.* 3, e2021AV000470.

Cabanes, C., Thierry, V., and Lagadec, C. (2016). Improvement of bias detection in Argo float conductivity sensors and its application in the North Atlantic. *Deep-Sea Res. Part I: Oceanographic Res. Papers* 114, 128–136. doi: 10.1016/j.dsr.2016.05.007

Cazenave, A., Hamlington, B., Horwath, M., Barletta, V. R., Benveniste, J., Chambers, D., et al. (2019). Observational requirements for long-term monitoring of the global mean sea level and its components over the altimetry era. *Front. Mar. Sci.* 6 (582). doi: 10.3389/fmars.2019.00582

Chamberlain, M. A., Oke, P. R., Fiedler, R. A. S., Beggs, H. M., Brassington, G. B., and Divakaran, P. (2021). Next generation of Bluelink ocean reanalysis with multiscale data assimilation: BRAN2020. *Earth Syst. Sci. Data Discuss* 13, 5663–5688. doi: 10.5194/essd-2021-194

Chang, L., Tang, H., Wang, Q., and Sun, W. (2019). Global thermosteric sea level change contributed by the deep ocean below 2000 m estimated by Argo and CTD data. *Earth Planetary Sci. Letters.* 524, 115727. doi: 10.1016/j.epsl.2019.115727

Chen, J., Cazenave, A., Dahle, C., Llovel, W., Panet, I., Pfeffer, J., et al. (2022). Applications and challenges of GRACE and GRACE follow-on satellite gravimetry. *Surveys Geophysics* 43, 305–345. doi: 10.1007/s10712-021-09685-x

Chen, J., Tapley, B., Wilson, C., Cazenave, A., Seo, K.-W., and Kim, J.-S. (2020). Global ocean mass change from GRACE and GRACE Follow-On and altimeter and Argo measurements. *Geophys. Res. Lett.* 47, e2020GL090656. doi: 10.1029/2020GL090656

Cimoli, L., Mashayek, A., Johnson, H. L., Marshall, D. P., Naveira Garabato, A. C., Whalen, C. B., et al. (2023). Significance of diapycnal mixing within the Atlantic meridional overturning circulation. *AGU Adv.* 4, e2022AV000800. doi: 10.1029/2022AV000800

Coppola, L., Prieur, L., Taupier-Letage, I., Estournel, C., Testor, P., Lefevre, D., et al. (2017). Observation of oxygen ventilation into deep waters through targeted deployment of multiple Argo-O_2 floats in the north-western Mediterranean Sea in 2013. *J. Geophys. Res.: Oceans* 122 (8), 6325–6341. doi: 10.1002/2016jc012594

de Boer, A. M., Hutchinson, D. K., Roquet, F., Sime, L. C., Burls, N. J., and Heuzé, C. (2022). The impact of southern ocean topographic barriers on the ocean circulation and the overlying atmosphere. *J. Climate* 35, 5805–5821. doi: 10.1175/JCLI-D-21-0896.1

Desbruyères, D. G., Bravo, E. P., Thierry, V., Mercier, H., Lherminier, P., Cabanes, C., et al. (2022). Warming-to-cooling reversal of overflow-derived water masses in the Irminger Sea during 2002–2021. *Geophysical Res. Lett.* 49, e2022GL098057. doi: 10.1029/2022GL098057

Desbruyères, D. G., Purkey, S. G., McDonagh, E. L., and Johnson, G. C. (2016). and King, B. A. Deep and abyssal ocean warming from 35 years of repeat hydrography. *Geophys. Res. Lett.* 43 (10), ,356–,310. doi: 10.1002/2016GL070413

Estapa, M. L., Breier, J. A., and German, C. R. (2015). Particle dynamics in the rising plume at Piccard Hydrothermal Field, Mid-Cayman Rise. *Geochem. Geophys. Geosyst.* 16, 2762–2774. doi: 10.1002/2015GC005831

Ferron, B., Bouruet Aubertot, P., Cuypers, Y., Schroeder, K., and Borghini, M. (2017). How important are diapycnal mixing and geothermal heating for the deep circulation of the Western Mediterranean? *Geophys. Res. Lett.* 44, 7845–7854. doi: 10.1002/2017GL074169

Ferron, B., Kokoszka, F., Mercier, H., and Lherminier, P. (2016). Variability of the diapycnal mixing along the A25 Greenland-Portugal transect repeated from 2002 to 2012. *J. Phys. Oceanography* 46, 1989–2003. doi: 10.1175/JPO-D-15-0186.1

Foppert, A., Rintoul, S. R., Purkey, S. G., Zilberman, N., Kobayashi, T., Sallèe, J.-B., et al. (2021). Deep Argo reveals bottom water properties and pathways in the Australian-Antarctic Basin. *J. Geophys. Res.: Oceans* 126, 1–18. doi: 10.1029/2021JC017935

Fox-Kemper, B., Hewitt, H. T., Xiao, C., Aðalgeirsdóttir, G., Drijfhout, S. S., Edwards, T. L., et al. (2021). "Cryosphere and sea level change," in *Climate change 2021: The Physical Science Basis. Contribution of Working Group I to the Sixth Assessment Report of the Intergovernmental Panel on Climate Change*. Eds. V. Masson-Delmotte, P. Zhai, A. Pirani, S. L. Connors, C. Péan, S. Berger, N. Caud, Y. Chen, L. Goldfarb, M. I. Gomis, M. Huang, K. Leitzell, E. Lonnoy, J. B. R. Matthews, T. K. Maycock, T. Waterfield, O. Yelekçi, R. Yu and B. Zhou (Cambridge, United Kingdom and New York, NY, USA: Cambridge University Press), 1211–1362. doi: 10.1017/9781009157896.011

Gaillard, F., Reynaud, T., Thierry, V., Kolodziejczyk, N., and von Schuckmann, K. (2016). *In-situ* based reanalysis of the global ocean temperature and salinity with ISAS: variability of the heat content and steric height. *J. Clim.* 29 (4), 1305–1323. doi: 10.1175/JCLI-D-15-0028.1

Garcia, H. E., Boyer, T. P., Baranova, O. K., Locarnini, R. A., Mishonov, A. V., Grodsky, A., et al. (2019). World ocean atlas 2018: product documentation. *A. Mishonov Tech. Editor*.

Garçon, V., Karstensen, J., Palacz, A., Telszewski, M., Aparco Lara, T., Breitburg, D., et al. (2019). Multidisciplinary observing in the world ocean's oxygen minimum zone regions: from climate to fish — The VOICE initiative. *Front. Mar. Sci.* 6. doi: 10.3389/fmars.2019.00722

Gardner, W. D., Richardson, M. J., Mishonov, A. V., and Biscaye, P. E. (2018). Global comparison of benthic nepheloid layers based on 52 years of nephelometer and transmissometer measurements. *Prog. Oceanogr* 168, 100–111. doi: 10.1016/j.pocean.2018.09.008

Gasparin, F., Guinehut, S., Mao, C., Mirouze, I., Rémy, E., King, R. R., et al. (2019). Requirements for an integrated in *situ* atlantic ocean observing system from coordinated observing system simulation experiments. *Front. Mar. Sci.* 6. doi: 10.3389/fmars.2019.00083

Gasparin, F., Hamon, M., Rémy, E., and Le Traon, P. (2020). How deep argo will improve the deep ocean in an ocean reanalysis. *J. Clim* 33 (1), 77–94. doi: 10.1175/JCLI-D-19-0208.1

GEBCO Bathymetric Compilation Group (2022). The GEBCO_2022 Grid - a continuous terrain model of the global oceans and land. *NERC EDS Br. Oceanographic Data Centre NOC*. doi: 10.5285/e0f0bb80-ab44-2739-e053-6c86abc0289c

Gordon, C., Fennel, K., Richards, C., Shay, L. K., and Brewster, J. K. (2020). Can ocean community production and respiration be determined by measuring high-frequency oxygen profiles from autonomous floats? *Biogeosciences* 17, 4119–4134. doi: 10.5194/bg-17-4119-2020

Grégoire, M., Garçon, V., Garcia, H., Breitburg, D., Isensee, K., Oschlies, A., et al. (2021). A global ocean oxygen database and atlas for assessing and predicting deoxygenation and ocean health in the open and coastal ocean. *Front. Mar. Sci.* 8. doi: 10.3389/fmars.2021.724913

Hu, L., Zhang, X., and Perry, M. J. (2019). Light scattering by pure seawater: Effect of pressure. *Deep Sea Res. Part I: Oceanographic Res. Papers* 146, 103–109. doi: 10.1016/j.dsr.2019.03.009

Hughes, K., Moum, J. N., and Rudnick, D. (2023). A turbulence data reduction scheme for autonomous and expendable profiling floats. *Ocean Sci.* 19, 193–207. doi: 10.5194/os-19-193-2023

Johnson, G. C. (2008). Quantifying antarctic bottom water and north atlantic deep water volumes. *J. Geophys. Res. Oceans* 113 (C5), 13. doi: C0502710.1029/2007jc004477

Johnson, G. C. (2022). Antarctic bottom water warming and circulation slowdown in the argentine basin from analyses of deep argo and historical shipboard temperature data. *Geophys. Res. Lett.* 49, e2022GL100526. doi: 10.1029/2022GL100526

Johnson, G. C., and Lyman, J. (2020). Warming trends increasingly dominate global ocean. *Nat. Clim. Change* 10, 757–761. doi: 10.1038/s41558-020-0822-0

Johnson, G. C., Cadot, C., Lyman, J., McTaggart, K. E., and Steffen, E. L. (2020). Antarctic bottom water warming in the Brazil basin: 1990s through 2020, from WOCE to deep argo. *Geophys. Res. Lett.* doi: 10.1029/2020GL089191

Johnson, G. C., Lyman, J. M., and Purkey, S. G. (2015). Informing deep argo array design using argo and full-depth hydrographic section data. *J. Atmos. Oceanic Technol.* 32, 2187–2198. doi: 10.1175/JTECH-D-15-0139.1

Johnson, G. C., Purkey, S. G., Zilberman, N. V., and Roemmich, D. (2019). Deep argo quantifies bottom water warming rates in the southwest pacific basin. *Geophys. Res. Lett.* 46, 2662–2669. doi: 10.1029/2018GL081685

Katsumata, K., Purkey, S. G., Cowley, R., Sloyan, B. M., Diggs, S. C., Moore, T. S., et al. (2022). GO-SHIP Easy Ocean: Gridded ship-based hydrographic section of temperature, salinity, and dissolved oxygen. *Sci. Data* 9, 103. doi: 10.1038/s41597-022-01212-w

Kobayashi, T., Sato, K., and King, B. A. (2021). Observed features of salinity bias with negative pressure dependency for measurements by SBE 41CP and SBE 61 CTD sensors on deep profiling floats. *Progr. Oceanogr.* 198, 102686. doi: 10.1016/j.pocean.2021.102686

Kobayashi, T., Watanabe, K., and Tachikawa, M. (2013). Deep NINJA collects profiles down to 4,000 meters. *Sea Technology.* 54, 41–44.

Kolodziejczyk, N., Prigent-Mazella, A., and Gaillard, F. (2021). *SEANOE*. doi: 10.17882/52367

Kwiatkowski, L., Torres, O., Bopp, L., Aumont, O., Chamberlain, M., Christian, J., et al. (2020). Twenty-first century ocean warming, acidification, deoxygenation, and upper ocean nutrient decline from CMIP6 model projections. *Biogeosciences* 17 (13), 3439–3470. doi: 10.5194/bg-17-3439-2020

Lam, P. J., and Bishop, J. K. B. (2008). The continental margin is a key source of iron to the HNLCNorth Pacific Ocean. *Geophys. Res. Lett.* 35. doi: 10.1029/2008GL033294

Le Boyer, A. (2021). Modular, flexible, low-cost microstructure measurements: the Epsilometer. *J. Atmos. Oceanic Technol.* 38 (3), 657–668. doi: 10.1175/JTECH-D-20-0116.1

Lele, R., Purkey, S. G., Nash, J. D., MacKinnon, J. A., Thurnherr, A. M., Whalen, C. B., et al. (2021). Abyssal heat budget in the southwest pacific basin. *J. Phys. Oceanogr.* 51 (11), 3317–3333. doi: 10.1175/JPO-D-21-0045.1

Lellouche, J.-M., Greiner, E., Bourdallé-Badie, R., Garric, G., Melet, A., Drévillon, M., et al. (2021). The copernicus global 1/12° Oceanic and sea ice GLORYS12 reanalysis. *Front. Earth Sci.* 9. doi: 10.3389/feart.2021.698876

Le Reste, S., Dutreuil, V., André, X., Thierry, V., Renaut, C., Le Traon, P.-Y., et al. (2016). Deep-Arvor: A new profiling float to extend the Argo observations down to 4000-m depth. *J. Atmos. Oceanic Technol.* 33, 1039–1055. doi: 10.1175/JTECH-D-15-0214.1

Levin, L. A. (2018). Manifestation, drivers, and emergence of open ocean deoxygenation, annu. *Rev. Mar. Sci.* 10 (1), 229–260. doi: 10.1146/annurev-marine-121916-063359

Levin, L. A., Bett, B. J., Gates, A. R., Heimbach, P., Howe, B. M., Janssen, F., et al. (2019). Global observing needs in the deep ocean. *Front. Mar. Sci.* 6. doi: 10.3389/fmars.2019.00241

Li, Q., England, M. H., Hogg, A. M., Rintoul, S. R., and Morrison, A. K. (2023). Abyssal ocean overturning slowdown and warming driven by Antarctic meltwater. *Nature* 615 (7954), 841–847. doi: 10.1038/s41586-023-05762-w

Llovel, W., Purkey, S., Meyssignac, B., Blazquez, A., Kolodziejczyk, N., and Bamber, J.. (2019). Global ocean freshening, ocean mass increase and global mean sea level rise over 2005–2015. *Sci. Rep.* 9, 17717. doi: 10.1038/s41598-019-54239-2

Loeb, N. G., Johnson, G. C., Thorsen, T. J., Lyman, J. M., Rose, F. G., and Kato, S. (2021). Satellite and ocean data reveal marked increase in earth's heating rate. *Geophys. Res. Lett.* 48e2021GL093047. doi: 10.1029/2021GL093047

MacKinnon, J. A., Zhao, Z., Whalen, C. B., Waterhouse, A. F., Trossman, D. S., Sun, O. M., et al. (2017). Climate process team on internal wave-driven ocean mixing. *Bull. Am. Meteorol. Soc.* 98, 2429–2454. doi: 10.1175/BAMS-D-16-0030.1

Martyr-Koller, R., Thomas, A., Schleussner, C. F., Nauels, A., and Lissner, T. (2021). Loss and damage implications of sea-level rise on Small Island Developing States. *Curr. Opin. Environ. Sustain* 50, 245–259. doi: 10.1016/j.cosust.2021.05.001

Mashayek, A., Ferrari, R., Merrifield, S., Ledwell, J. R., St Laurent, L., Naveira Garabato, A., et al. (2017). Topographic enhancement of vertical turbulent mixing in the Southern Ocean. *Nat. Commun.* 8, 14197. doi: 10.1038/ncomms14197

Mayer, L. A., Jakobsson, M., Allen, G., Dorschel, B., Falconer, R., Ferrini, V., et al. (2018). The nippon foundation—GEBCO seabed 2030 project: the quest to see the world's oceans completely mapped by 2030. *Geosciences* 8, 63. doi: 10.3390/geosciences8020063

Meyssignac, B., Boyer, T., Zhao, Z., Hakuba, M. Z., Landerer, F. W., Stammer, D., et al. (2019). Measuring global ocean heat content to estimate the Earth energy imbalance. *Front. Mar. Sci.* 6, 432. doi: 10.1002/2015JC011288

Nagai, T., Inoue, R., Tandon, A., and Yamazaki, H. (2015). Evidence of enhanced double-diffusive convection below the main stream of the Kuroshio Extension. *J. Geophys. Res. Oceans* 120, 8402–8421. doi: 10.1002/2015JC011288

Nerem, R. S., Beckley, B. D., Fasullo, J. T., Hamlington, B. D., Masters, D., and Mitchum, G. T. (2018). Climate-change–driven accelerated sea-level rise detected in the altimeter era. *Proc. Natl. Acad. Sci.* 115 (9), 2022–2025. doi: 10.1073/pnas.1717312115

Ollitrault, M., and Rannou, J.-P. (2013). ANDRO: an argo-based deep displacement dataset. *J. Atmos. Ocean. Technol.* 30 (4), 759–788. doi: 10.1175/JTECH-D-12-00073.1

Oschlies, A., Brandt, P., and Stramma, L. (2018). and Schmidtko, S. Drivers and mechanisms of ocean deoxygenation. *Nat. Geosci.* 11 (7), 467–473. doi: 10.1038/s41561-018-0152-2

Owens, W. B., and Wong, A. P. S. (2009). An improved calibration method for the drift of the conductivity sensor on autonomous CTD profiling floats by ⊖-S climatology. *Deep-Sea Res. Part I* 56, 450–457. doi: 10.1016/j.dsr.2008.09.008

Owens, W. B., Zilberman, N., Johnson, K. S., Claustre, H., Scanderbeg, M., Wijffels, S., et al. (2022). OneArgo: A new paradigm for observing the global ocean. *Mar. Technol. Soc J.* 56 (3), 84–90. doi: 10.4031/MTSJ.56.3.8

Palmer, M. D. (2017). Reconciling estimates of ocean heating and earth's radiation budget. *Curr. Clim. Change Rep.* 3, 78–86. doi: 10.1007/s40641-016-0053-7

Palmer, M. D., McNeall, D. J., and Dunstone, N. J. (2011). Importance of the deep ocean for estimating decadal changes in Earth's radiation balance. *Geophys. Res. Lett.* 38, L13707. doi: 10.1029/2011GL047835

Passarelli, L., Cesca, S., Nooshiri, N., and Jónsson, S. (2022). Earthquake fingerprint of an incipient subduction of a bathymetric high. *Geophys. Res. Lett.* 49, e2022GL100326. doi: 10.1029/2022GL100326

Petit, T., Thierry, V., and Mercier, H. (2022). Deep through-flow in the bight fracture zone. *Ocean Sci.* 18, 1055–1071. doi: 10.5194/os-18-1055-2022

Petzrick, E., Truman, J., and Fargher, H. (2014). *Profiling from 6000 meter with the APEX-Deep float*. 2013 OCEANS - San Diego, CA, USA, (2013) pp. 1–3. doi: 10.23919/OCEANS.2013.6741074

Piron, A., Thierry, V., Mercier, H., and Caniaux, G. (2016). Observation of basin-scale deep convection in the Irminger Sea with Argo floats in the 2011-2012 winter. *Deep-Sea Res. Part I* 109, 76–90. doi: 10.1016/j.dsr.2015.12.012

Purkey, S. G., and Johnson, G. C. (2010). Warming of Global Abyssal and Deep Southern Ocean waters between the 1990s and 2000s: Contributions to global heat and sea level rise budgets. *J. Clim* 23 (23), 6336–6351. doi: 10.1175/2010JCLI3682.1

Purkey, S. G., Johnson, G. C., Talley, L. D., Sloyan, B. M., Wijffels, S. E., Smethie, W., et al. (2019). Unabated bottom water warming and freshening in the South Pacific Ocean. *J. Geophys. Res. Oceans* 124 (3), 1778–1794. doi: 10.1029/2018jc014775

Racapé, V., Thierry, V., Mercier, H., and Cabanes, C. (2019). ISOW spreading and mixing as revealed by Deep-Argo floats launched in the Charlie-Gibbs Fracture Zone. *J. Geophys. Res.: Oceans* 124, 6787–6808. doi: 10.1029/2019JC015040

Ray, D., KameshRaju, K. A., Srinivas Rao, A., et al. (2020). Elevated turbidity and dissolved manganese in deep water column near 10°47'S Central Indian Ridge: studies on hydrothermal activities. *Geo-Mar. Lett.* 40, 619–628. doi: 10.1007/s00367-020-00657-5

Riser, S., and Johnson, K. (2008). Net production of oxygen in the subtropical ocean. *Nature* 451, 323–325. doi: 10.1038/nature06441

Roemmich, D., Alford, M. H., Claustre, H., Johnson, K., King, B., Moum, J., et al. (2019a). On the future of argo: A global, full-depth, multi-disciplinary array. *Front. Mar. Sci.* 6. doi: 10.3389/fmars.2019.00439

Roemmich, D., Sherman, J. T., Davis, R. E., Grindley, K., McClune, M., Parker, C. J., et al. (2019b). Deep SOLO: A full-depth profiling float for the Argo Program. *J. Atmos. Oceanic Technol.* 36 (10), 1967–1981. doi: 10.1175/jtech-d-19-0066.1

Royston, S., Vishwakarma, B. D., Westaway, R. M., Rougier, J., Sha, Z., and Bamber, J. L. (2020). Can we resolve the basin-scale sea level trend budget from GRACE ocean mass? *J. Geophys. Res.: Oceans* 125, e2019JC015535. doi: 10.1029/2019JC015535

Salaree, A., and Okal, E. A. (2020). Effects of bathymetry complexity on tsunami propagation: a spherical harmonics approach. *Geophys. J. Int.* 223 (1), 632–647. doi: 10.1093/gji/ggaa334

Sauzède, R., Bittig, H. C., Claustre, H., Pasqueron de Fommervault, O., Gattuso, J.-P., Legendre, L., et al. (2017). Estimates of water-column nutrient concentrations and carbonate system parameters in the global ocean: A novel approach based on neural networks. *Front. Mar. Sci.* 4. doi: 10.3389/fmars.2017.00128

Schmidtko, S., Stramma, L., and Visbeck, M. (2017). Decline in global oceanic oxygen content during the past five decades. *Nature* 542, 335–339. doi: 10.1038/nature21399

Séférian, R., Berthet, S., Yool, A., Palmiéri, J., Bopp, L., Tagliabue, A., et al. (2020). Tracking improvement in simulated marine biogeochemistry between CMIP5 and CMIP6. *Curr. Clim. Change Rep.* 6, 95–119. doi: 10.1007/s40641-020-00160-0

Sévellec, F., and Fedorov, A. V. (2013). Model bias reduction and the limits of oceanic decadal predictability: Importance of the deep ocean. *J. Climate* 26, 3688–3707. doi: 10.1175/JCLI-D-12-00199.1

Stammer, D., Bracco, A., AchutaRao, K., Beal, L., Bindoff, N. L., Braconnot, P., et al. (2019). Ocean climate observing requirements in support of climate research and climate information. *Front. Mar. Sci.* 6. doi: 10.3389/fmars.2019.00444

Swingedouw, D., Houssais, M.-N., Herbaut, C., Blaizot, A.-C., Devilliers, M., and Deshayes, J. (2022). AMOC recent and future trends: A crucial role for oceanic resolution and Greenland melting? *Front. Clim.* 4. doi: 10.3389/fclim.2022.838310

Testor, P., Bosse, A., Houpert, L., Margirier, F., Mortier, L., Legoff, H., et al. (2018). Multiscale observations of deep convection in the northwestern mediterranean sea during winter 2012–2013 using multiple platforms. *J. Geophys. Res.: Oceans* 123, 1745–1776. doi: 10.1002/2016JC012671

Thomas, G., Purkey, S. G., Roemmich, D., Foppert, A., and Rintoul, S. R. (2020). Spatial variability of antarctic bottom water in the Australian antarctic basin from 2018-2020 captured by deep argo. *Geophys. Res. Lett.* 47. doi: 10.1029/2020gl089467

Tozer, B., Sandwell, D. T., Smith, W. H. F., Olson, C., Beale, J. R., and Wessel, P. (2019). Global bathymetry and topography at 15 arc sec: SRTM15+. *Earth Space Sci.* 6, 1847–1864. doi: 10.1029/2019EA000658

Ulses, C., Estournel, C., Fourrier, M., Coppola, L., Kessouri, F., Lefèvre, D., et al. (2021). Oxygen budget of the north-western Mediterranean deep-convection region. *Biogeosciences* 18, 937–960. doi: 10.5194/bg-18-937-2021

Uotila, P., Goosse, H., Haines, K., Chevallier, M., Barthélemy, A., Bricaud, C., et al. (2019). An assessment of ten ocean reanalyses in the polar regions. *Clim. Dyn.* 52, 1613–1650. doi: 10.1007/s00382-018-4242-z

van Wijk, E. M., Hally, B., Wallace, L. O., Zilberman, N., and Scanderbeg, M. (2022). Can Argo floats help improve bathymetry? *Int. Hydrographic Rev.* 28, 226–230. doi: 10.58440/ihr-28-n08

van Wijk, E. M., and Rintoul., S. R. (2014). Freshening drives contraction of Antarctic Bottom Water in the Australian Antarctic Basin. *Geophys. Res. Lett.* 41 (5), 1657–1664. doi: 10.1002/2013gl058921

Vladoiu, A., Bouruet-Aubertot, P., Cuypers, Y., Ferron, B., Schroeder, K., Borghini, M., et al. (2021). Contrasted mixing efficiency in energetic versus quiescent regions: insights from microstructure measurements in the Western Mediterranean Sea. *Prog. Oceanogr.* 195, 102594. doi: 10.1016/j.pocean.2021.102594

von Schuckmann, K., Cheng, L., Palmer, M. D., Hansen, J., Tassone, C., Aich, V., et al. (2020). Heat stored in the Earth system: where does the energy go? *Earth Syst. Sci. Data* 12, 2013–2041. doi: 10.5194/essd-12-2013-2020

von Schuckmann, K., Minère, A., Gues, F., Cuesta-Valero, F. J., Kirchengast, G., Adusumilli, S., et al. (2023). Heat stored in the Earth system 1960–2020: Where does the energy go? *Earth Syst. Sci. Data Discuss* 15, 1675–1709. doi: 10.5194/essd-15-1675-2023

Walicka, K., King, B., Thierry, V., Cabanes, C., Vélez-Belchí, P., Coatanoan, C., et al. (2022). D3.4: Report of the outcome of the comparative study for the deep Argo quality control processing. *Zenodo*. doi: 10.5281/zenodo.8366455

Waterhouse, A. F., MacKinnon, J. A., Nash, J. D., Alford, M. H., Kunze, E., Simmons, H. L., et al. (2014). Global patterns of diapycnal mixing from measurements of the turbulent dissipation rate. *J. Phys. Oceanogr* 44 (7), 1854–1872. doi: 10.1175/JPO-D-13-0104.1

WCRP Global Sea Level Budget Group (2018). Global sea-level budget 1993–present. *Earth Syst. Sci. Data* 10, 1551–1590. doi: 10.5194/essd-10-1551-2018

Whalen, C. B., MacKinnon, J. A., and Talley, L. D. (2015). and Waterhouse, A. F. Estimating the mean diapycnal mixing using a finescale strain parameterization. *J. Phys. Oceanogr.* 45, 1174–1188. doi: 10.1175/JPO-D-14-0167.1

Whalen, C. B., Talley, L. D., and MacKinnon, J. A. (2012). Spatial and temporal variability of global ocean mixing inferred from Argo profiles. *Geophys. Res. Lett.* 39. doi: 10.1029/2012gl053196

Wilson, E. A., Thompson, A. F., Stewart, A. L., and Sun, S. (2022). Bathymetric control of subpolar gyres and the overturning circulation in the southern ocean. *J. Phys. Oceanogr* 52 (2), 205–223. doi: 10.1175/JPO-D-21-0136.1

Wölfl, A.-C., Snaith, H., Amirebrahimi, S., Devey, C. W., Dorschel, B., Ferrini, V., et al. (2019). Seafloor mapping – the challenge of a truly global ocean bathymetry. *Front. Mar. Sci.* 6. doi: 10.3389/fmars.2019.00283

Wong, A. P. S., Wijffels, S. E., Riser, S. C., Pouliquen, S., Hosoda, S., Roemmich, D., et al. (2020). Argo data 1999-2019: two million temperature-salinity profiles and subsurface velocity observations from a global array of profiling floats. *Front. Mar. Sci.* 7. doi: 10.3389/fmars.2020.00700

Yashayaev, I. (2007). Hydrographic changes in the labrador se-2005. *Prog. Oceanogr* 73 (3-4), 242–276. doi: 10.1016/j.pocean.2007.04.015

Zhang, H. L. J., Whalen, C. B., Kumar, N., and Purkey, S. G. (2021). Decreased stratification in the abyssal southwest pacific basin and implications for the energy budget. *Geophys. Res. Lett.* 48 (19). doi: 10.1029/2021gl094322

Zhou, S., Meijers, A. J. S., Meredith, M. P., Povl Abrahamsen, E., Holland, P. R., Silvano, A., et al. (2023). Slowdown of Antarctic Bottom Water export driven by climatic wind and sea-ice changes. *Nat. Clim. Chang.* 13, 701–709. doi: 10.1038/s41558-023-01695-4

Zilberman, N., King, B., Purkey, S., Thierry, V., and Roemmich, D. (2019). *Report on the 2nd Deep Argo Implementation Workshop* (Hobart). Available at: https://archimer.ifremer.fr/doc/00507/61873/.

Zilberman, N. V., Roemmich, D. H., and Gilson., J. (2020). Deep-ocean circulation in the southwest pacific ocean interior: estimates of the mean flow and variability using deep argo data. *Geophys. Res. Lett.* 47, (13). doi: 10.1029/2020gl088342

Zilberman, N. V., Scanderbeg, M., Gray, A. R., and Oke, P. R. (2023). Scripps Argo trajectory-based velocity product: global estimates of absolute velocity derived from core, biogeochemical, and deep argo float trajectories at parking depth. *J. Atmos. Oceanic Technol.* 40 (3), 361–374. doi: 10.1175/JTECH-D-22-0065.1